Estimation of Space and Time Evolution of Mg^{2+} Concentration near a Mg^{2+}-Releasing Implant

Sandor Nemeth [1][0000-0001-8164-8797] and Clarice Loke [2][0009-0002-3482-4895]

Singapore Institute of Manufacturing Technology (SIMTech), Agency for Science, Technology and Research (A*STAR), Republic of Singapore
[1] sandorn@simtech.a-star.edu.sg
[2] phloke@simtech.a-star.edu.sg

Abstract. According to literature reports based on *in vitro* tests, transient increase in Mg^{2+} concentration to 2 to 10 mM can promote osteogenesis around implants. However, it is not well established how the Mg^{2+} concentration may change in space and time around a Mg^{2+}-releasing implant *in vivo*, and whether therapeutic levels of Mg^{2+} can be maintained in the surrounding tissues. Thus, the temporal and spatial evolution of Mg^{2+} concentration was investigated from a $MgSO_4 \cdot 7H_2O$ containing polycaprolactone implant by numerical analysis using a rudimentary diffusion model. Diffusion coefficient of Mg^{2+} in polycaprolactone was determined experimentally, while it was estimated in body fluids and tissue from literature data. The results revealed that Mg^{2+} levels generally increase modestly and reach the therapeutic level for less than one day in this system due to fast clearing of Mg^{2+} from the tissues. Toxic levels of Mg^{2+} concentration may develop, but only for a few minutes, and can be mitigated by a thin layer of pure polymer applied on the implant.

Keywords: Polycaprolactone, Implant, Magnesium release, Osteogenesis.

1 Introduction

Magnesium is an essential element in living organisms, and it is known to be involved in a large number of biochemical pathways [1]. One important role of Mg^{2+} is found in osteogenesis. It has been reported that elevated Mg^{2+} levels can accelerate osteogenesis and angiogenesis via varied mechanism if the magnesium concentration is well above the physiological level (0.65 mM – 1.05 mM), somewhere in the optimal range of 2 mM to 10 mM as determined by *in vitro* experiments [2]. To take advantage of these positive effects of magnesium in regenerative medicine with regards to bone injuries, a suitable approach is to implant a temporary scaffold that can release Mg^{2+} at the site of implantation. This is to increase the magnesium concentration locally for a suitable duration and guide accelerated bone development. However, the duration of elevated magnesium level should not be excessively long as high concentration of magnesium can inhibit the mineralization process in the later stages of bone development.

The *in vitro* experiments reported in the literature are static with regards to the magnesium concentration, and it is an open question how these results may be used *in vivo* where the interplay between the release rate of Mg^{2+} from the scaffold, and its clearing from the vicinity of the implant creates a dynamic concentration profile [2]. Although this concentration profile could potentially be evaluated via experimental methods, the method would be complicated and difficult to plan and implement. Thus, the authors conducted numerical simulation studies as a first step to evaluate the likely fate of magnesium that is released from an implant material. A rudimentary model was used in the calculations with several simplifications that may preclude highly reliable quantitative results, but it is suitable to evaluate the main factors responsible for the release profile that one may expect. Thus, the outcome from the calculations could be used to guide the design of more sophisticated calculations and experiments while providing basic insights into magnesium release profile from an implant. The study focused on the release of magnesium sulphate from polycaprolactone (PCL) carrier since PCL is used as a biodegradable temporary implant for bone regeneration.

2 Model Setup

2.1 Geometry

A very simple release geometry was used as shown in Fig. 1 consisting of a sheet of PCL loaded with $MgSO_4 \cdot 7H_2O$, an optional layer of Mg^{2+}-free PCL, body fluid layer, tissue layer and a magnesium sink (microcapillaries). The thickness of the PCL and body fluid layers were selected arbitrarily while the tissue layer was selected based on capillary density in living tissue (see Table 1). For viability, cells can be only from a limited distance from capillaries. This can be as low as about 15 µm in mouse brain tissue [3] or as much as 67.2 ± 25.3 µm capillary-free zone in human retina [4]. Thus, the tissue layer thickness was varied in the comparable 20 µm to 80 µm range. The model was simplified by assuming the tissue to be a uniform and homogeneous layer (no cellular structure) for the purpose of magnesium transport.

All the layers were divided into 1 µm thick sub layers for the purpose of calculating changes in magnesium concentration.

2.2 Initial Mg^{2+} Concentrations

The concentration of $MgSO_4 \cdot 7H_2O$ in the PCL implant material was selected at two levels, 480 mM and 990 mM, approximately corresponding 10 w% and 20 w% salt in the polymer composite. Further, it was assumed that the salt is distributed homogeneously in the implant. When a pure PCL coating layer was considered on the implant, it had 0 mM initial salt content. The body fluid and tissue had 1 mM initial magnesium concentration, while the capillaries always had a fixed 1 mM magnesium concentration.

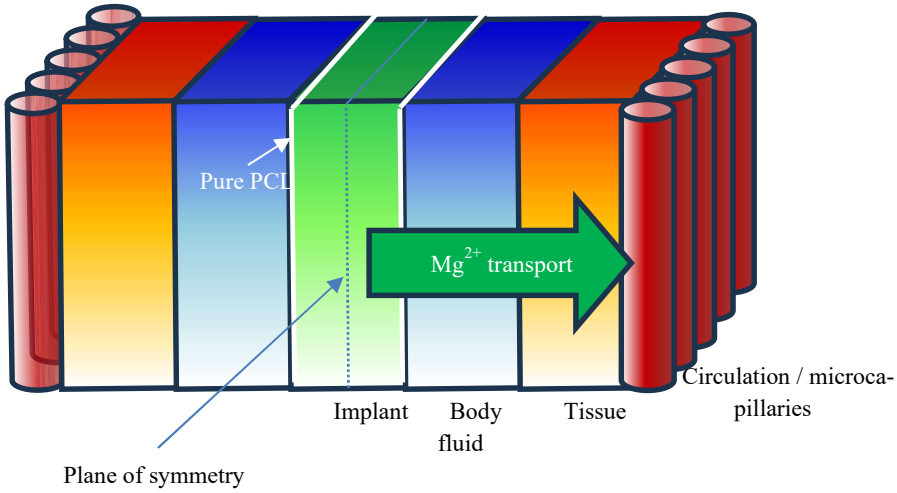

Fig. 1. Geometric arrangement of the model: Implant is a large sheet of PCL containing $MgSO_4 \cdot 7H_2O$ that is optionally coated with a layer of pure PCL. The implant is in contact with body fluid followed by a layer of tissue. Finally, microcapillaries are present that transport the excess magnesium away from the implant area. The transport is one dimensional; the setup is symmetric, and calculation is done only for half of the system.

2.3 Diffusion Coefficients

The numerical model relied solely on simple diffusional transport of magnesium from the implant to the capillaries. The numerical value of diffusion coefficient of $MgSO_4$ in the presence of water was determined in PCL experimentally and described in a conference presentation [5]. Briefly, PCL (M=80,000 g/mol) was loaded with approximately 20w% $MgSO_4 \cdot 7H_2O$ by cryo-milling the polymer pellets with sieved salt crystals to exclude sizes above 45 µm. The resulting powder was then extruded to form filaments with varied radii. Additionally, flat samples of varied thickness were made from filaments by pressing the material between two flat surfaces lined with PTFE sheets above the melting point of PCL. The release of Mg^{2+} into water was then measured at 37°C using electrical conductivity. The resulting release profile was fitted to theoretical diffusion driven release profiles [6] using least squares optimization. However, it was found that the release of $MgSO_4$ did not follow a simple diffusion process, and it was necessary to assume two parallel processes with two distinct diffusion coefficients. Thus, equation 1 was used to fit the magnesium release from filament samples and equation 2 for sheet samples by combining two parallel diffusion processes.

$$F_c(t) = 1 - f_1 \sum_{n=1}^{\infty} \frac{4}{R^2 \alpha_n^2} e^{-D_1 \alpha_n^2 t} - f_2 \sum_{n=1}^{\infty} \frac{4}{R^2 \alpha_n^2} e^{-D_2 \alpha_n^2 t} \quad (1)$$

$$F_s(t) = 1 - f_1 \sum_{n=0}^{\infty} \frac{8}{(2n+1)^2 \pi^2} e^{-\frac{D_1 (2n+1)^2 \pi^2 t}{4L^2}} - f_2 \sum_{n=0}^{\infty} \frac{8}{(2n+1)^2 \pi^2} e^{-\frac{D_2 (2n+1)^2 \pi^2 t}{4L^2}} \quad (2)$$

where F_c is the release profile over time (t) for filament (cylinder) and F_s for sheet, expressed as cumulative Mg^{2+} fraction released. R is the radius of the filament, α_n is defined through $J_0(R\alpha_n) = 0$, where J_0 is the zeroth order Bessel function of the first kind. D_1 and D_2 are the two diffusion coefficients, and f_1 and f_2 are the corresponding fraction of magnesium released through processes associated with D_1 and D_2, respectively. L is the half-thickness of the sheet. The fitting was carried out by truncating the infinite sums to a number of terms such that use of additional terms gave negligible contribution to the sums.

It was found that the recovered fitting parameters D_1 and D_2 as well as f_1 and f_2 were reasonably consistent across different sample shapes and sample radius / thickness. For filament samples (4 samples): $D_{1,c}$ = (4.8 ± 2.2) x10^{-9} cm^2/s, $D_{2,c}$ = (7.8 ± 2.1) x10^{-10} cm^2/s, $f_{1,c}$ = 0.77 ± 0.12, and $f_{2,c}$ = 0.23 ± 0.12. For sheet samples (4 samples): $D_{1,s}$ = (4.8 ± 0.4) x10^{-9} cm^2/s, $D_{2,s}$ = (5.5 ± 3.3) x10^{-10} cm^2/s, $f_{1,s}$ = 0.85 ± 0.05, and $f_{2,s}$ = 0.15 ± 0.05. Averaging over eight samples including both geometries and varied thickness/radius gave: $D_{1,avg}$ = (4.8 ± 1.4) x10^{-9} cm^2/s, $D_{2,avg}$ = (6.7 ± 2.8) x10^{-10} cm^2/s, $f_{1,avg}$ = 0.81 ± 0.10, and $f_{2,avg}$ = 0.19 ± 0.10.

To simplify the present simulation of Mg^{2+} release, only a single diffusion process was considered with diffusion coefficient rounded to D = 5 x10^{-9} cm^2/s, see Table 1. This is justifiable since approximately 80% of the magnesium sulphate is released through the faster diffusion process which is primarily responsible for the initial magnesium release that corresponds to the concentration elevation to the therapeutic range.

The diffusion coefficient of magnesium sulphate in body fluid was approximated by the value measured in water (~8 x10^{-6} cm^2/s at 25°C) [7]. This value is expected to be lowered somewhat by the elevated ionic strength in body fluid, while the higher temperature (37°C) would increase the value [8]. Since both effects result in moderate and opposing changes, they were ignored.

Reports on the diffusion coefficient of magnesium ions in tissue are rather rare. However, it was reported that magnesium has (1.88 ± 0.09) x10^{-6} cm^2/s intracellular diffusion coefficient in rat muscle fibers [9], and (2 to 3) x10^{-6} cm^2/s in barnacle muscle [10]. A similar value, 2x10^{-6} cm^2/s, was found in a very different tissue type of squid axon [11]. Based on the above reports, a diffusion coefficient of 2 x10^{-6} cm^2/s was used for magnesium transport through the tissue layer.

Table 1. Parameters used in the numerical simulation.

Layer	$D(Mg^{2+})$, cm^2/s	Initial Mg^{2+} concentration, mM	Layer thickness values used, μm
Implant	5x10^{-9}	480, 990	300, 600
PCL coating	5x10^{-9}	0	0, 10
Body fluid	8x10^{-6}	1	0, 10, 20, 50
Tissue	2x10^{-6}	1	20, 50, 80
Circulation	Not Applicable	1	Not Applicable

2.4 Numerical Simulation Method

A very simple method was used for the simulation as described by Crank in his book [6] in Chapter 8, Section 8.3. This consisted of calculating the change in concentrations for a small time step, τ, then updating the concentrations with the changes. To avoid divergence, the time step was selected such that $\tau < 0.5h^2/D$ where h is the layer thickness used as the distance step (h = 1 μm), and D is the diffusion coefficient in that layer. The calculation was carried out using Python code, and total time span was 87000 seconds.

3 Results

3.1 Influence of Layer Thickness Variations

It was found that the thicknesses of implant material, PCL coating on the implant, and tissue layer have significant influence on the evolution of magnesium concentrations within the tissue. On the other hand, the thickness of the body fluid layer, having the fastest magnesium diffusion, had small influence on the results. Thus, most of the results are presented for the case when the body fluid layer is the thickest (50 μm).

3.2 Evolution of Magnesium Concentration in the Implant

The change in magnesium concentration within the implant is shown in Fig. 2 for 480 mM initial Mg loading. The curves have the expected shapes based on diffusion theory [6]. Addition of 10 μm thick pure PCL layer has negligible effect on the overall evolution of concentrations except for limiting the maximum magnesium concentration on the surface in contact with the body fluid. This is also expected, as the presence of a pure PCL layer leads to a short lag time [12] that is sufficient to moderate the surface concentration since it provides time for the surroundings to take up magnesium as it is appearing on the surface from the implant.

Similarly, changing the layer thickness of body fluid and tissue in contact has negligible influence on the shape of the curves within the implant (not shown in the figure). Calculations using 990 mM initial concentration provided the same shape of curves as shown in Fig. 2, except the concentration values were higher, proportional to the initial magnesium concentration.

The effect of using a thicker PCL implant is significant. The amount of magnesium remaining in the implant after a given duration is much higher than in the case of thinner implant. However, the magnesium concentrations on the implant surface are comparable for thin and thick implants. Again, the results are in full agreement with theoretical equations [6].

3.3 Concentration Profiles in Body Fluid and Tissue

The calculated concentration profiles of Mg^{2+} over time at selected locations are plotted in Fig. 3 to 6 for different conditions. To limit the number of plots, only the cases

with 80 µm tissue thickness were include. The presence of thinner tissue layers accelerates the decrease of magnesium concentration over time. The locations plotted are body fluid in contact with the implant, tissue surface facing the implant, tissue middle layer, and tissue facing capillaries. Of these, the tissue surface in contact with the capillaries has insignificant magnesium concentration increase in all cases.

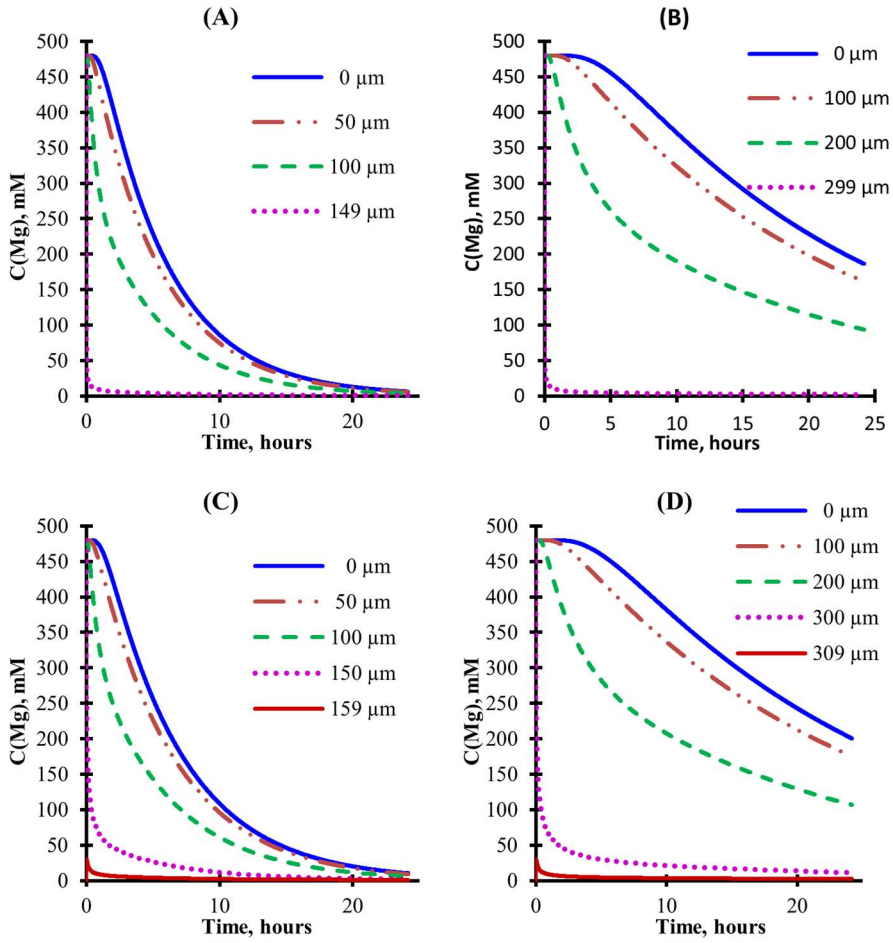

Fig. 2. Evolution of magnesium concentration within implant at different locations (center at 0 µm, surface at 149 µm or 299 µm) for 480 mM initial Mg^{2+} loading, 50 µm body fluid layer and 80 µm tissue layer. (A): No PCL coating is present, 300 µm thick implant. (B): No PCL coating is present, 600 µm thick implant. (C): 10 µm PCL coating without magnesium is present on 300 µm thick implant; concentration on coating layer surface rises fast to ~ 30 mM, then decays (lowest curve in plot). (D): 10 µm PCL coating without magnesium is present on 600 µm thick implant; concentration on coating layer surface rises fast to ~ 30 mM, then decays (lowest curve in plot).

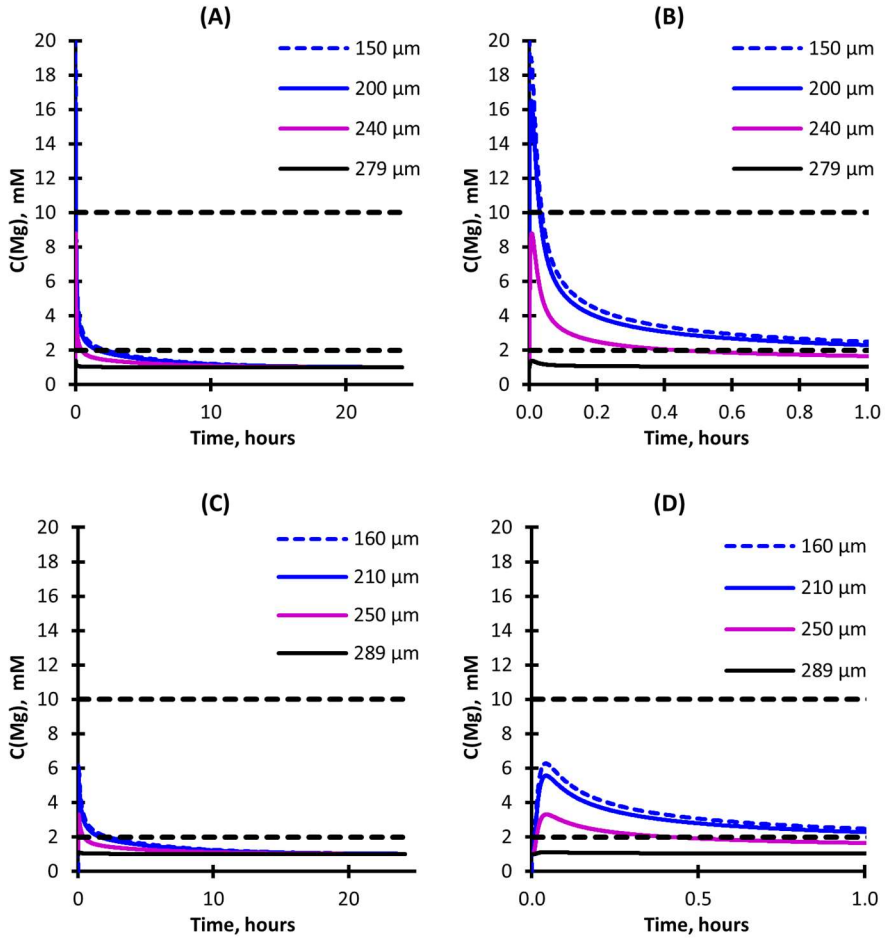

Fig. 3. Evolution of magnesium concentration in body fluid at the implant surface (dashed blue lines) and in tissue (solid lines indicating different locations). Implant thickness is 300 µm, salt content is 480 mM initial Mg^{2+} loading in implant. The optimum therapeutic concentration range is indicated by the black horizontal dashed lines. (A) and (B) with different time scales: No pure PCL coating on implant showing highly elevated magnesium level in the initial few minutes. (C) and (D) with different time scales: 10 µm pure PCL coating is present on the implant which significantly moderates the initial magnesium concentration rise, thus avoiding buildup of potentially toxic levels.

The time dependent concentration profiles indicate a very sharp rise in magnesium level within less than a minute if no pure PCL coating is present on the implant. If 10 µm PCL coating is added, the peak magnesium concentration is reached within about three minutes and this peak level is much lower than in the case where no PCL coat-

ing is in place. After the peak concentration is reached, the concentration drops quickly with time evolution resembling a decaying exponential function.

The effect of initial magnesium loading in the implant is the shifting of concentration values in proportion to the initial concentration without otherwise affecting the profiles (compare Fig. 3 and Fig. 4), as seen similarly in the case of concentrations within the implant.

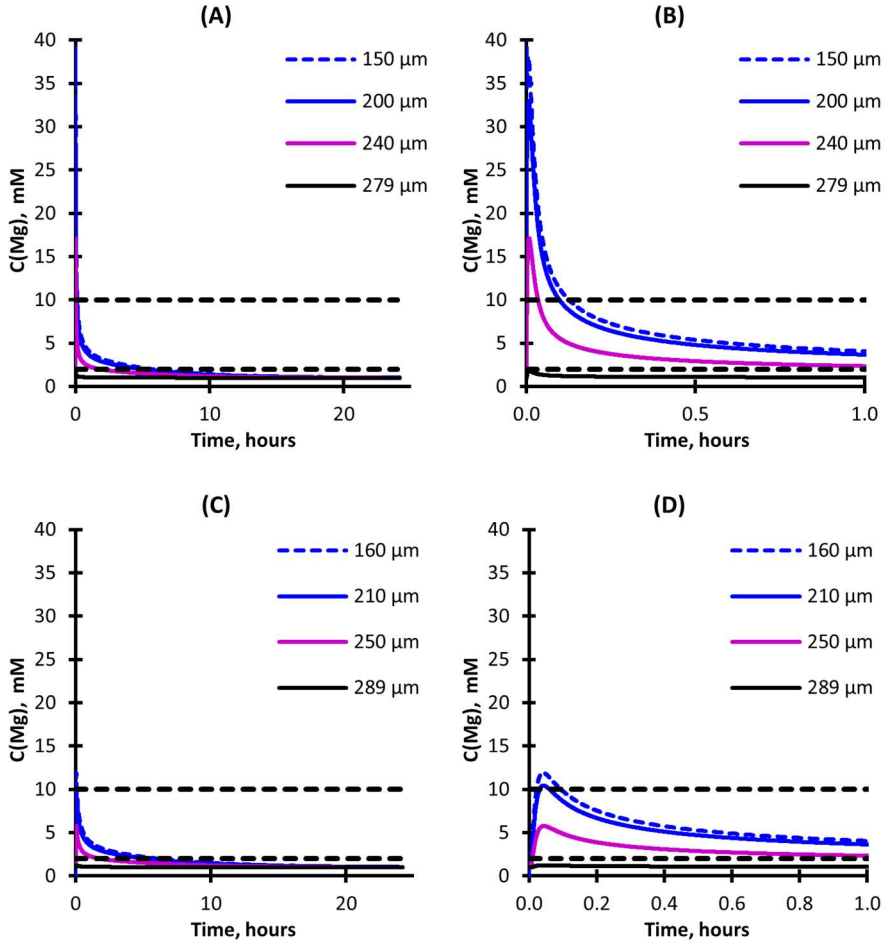

Fig. 4. Same conditions as in Fig. 3, except for the initial Mg^{2+} loading in the implant is 990 mM. The shapes of the curves are nearly identical to those in Fig. 3 except for the concentration values are higher in proportion to the initial loading level in the implant.

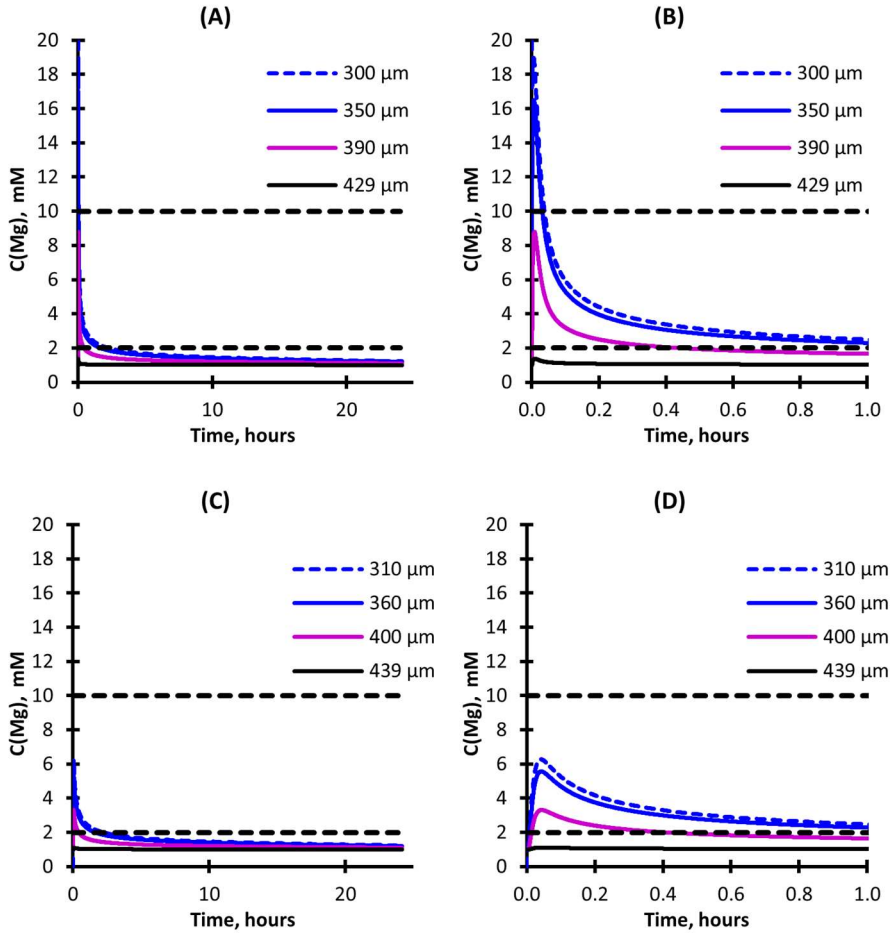

Fig. 5. Evolution of magnesium concentration in body fluid at the implant surface (dashed blue lines) and in tissue (solid lines indicating different locations). Implant thickness is 600 µm, salt content is 480 mM initial Mg^{2+} loading in implant. The optimum therapeutic concentration range is indicated by the black horizontal dashed lines. (A) and (B) with different time scales: No pure PCL coating on implant showing highly elevated magnesium level in the initial few minutes. (C) and (D) with different time scales: 10 µm pure PCL coating is present on the implant which significantly moderates the initial magnesium concentration rise, thus avoiding buildup of potentially toxic levels.

The thickness of the implant has no effect on the initial part of the concentration profiles since the initial magnesium release is determined by the magnesium concentration near the surface of the implant. However, as the magnesium content is depleted in the implant over time, the thinner material starts to supply a lesser amount of

magnesium while the thicker implant can supply more magnesium as it diffuses from the interior. Thus, thicker implant increases the magnesium concentration in the tissue layer at later times of the release.

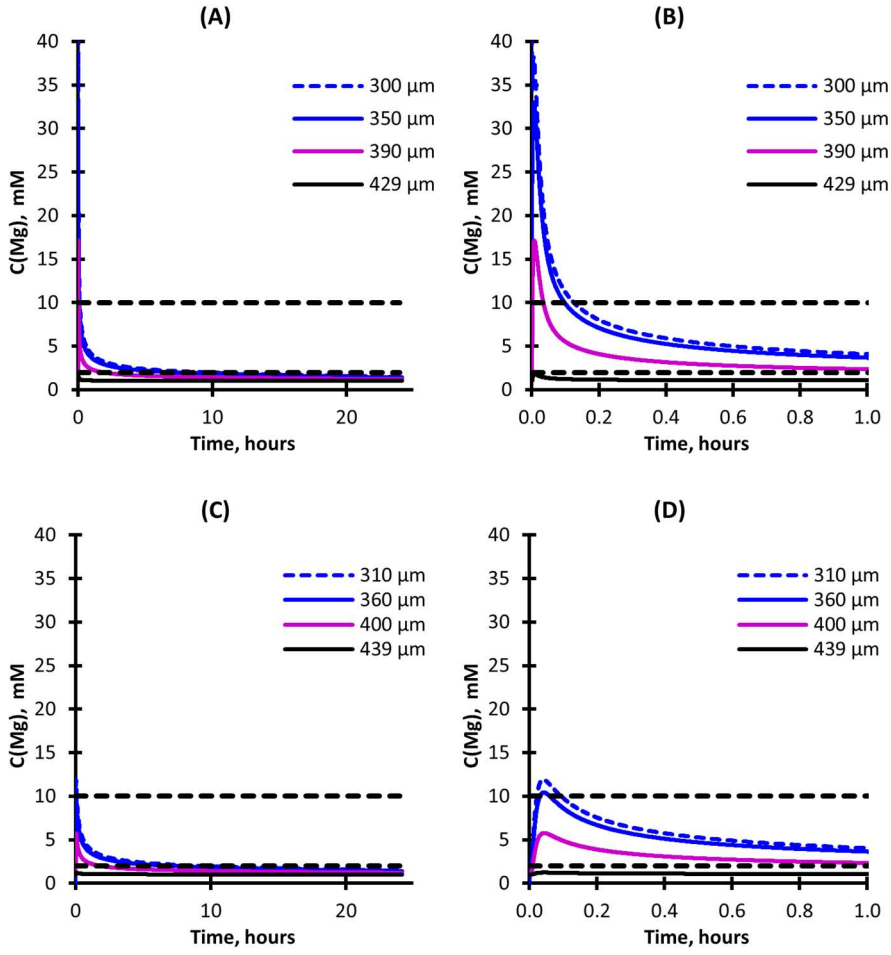

Fig. 6. Same conditions as in Fig. 5, except for the initial Mg^{2+} loading in the implant is 990 mM. The shapes of the curves are nearly identical to those in Fig. 5 except for the concentration values are higher in proportion to the initial loading level in the implant.

4 Discussion

The key parameters that can be obtained from the simulation are the duration of elevated magnesium concentration within the optimum therapeutic range (2 mM to 10

mM), and the duration of magnesium concentration exceeding the optimum therapeutic concentration which may potentially lead to toxic levels of Mg^{2+}. Since the thickness of the body fluid layer (0, 10, 20, and 50 μm) has little effect on the duration of elevated concentrations in the tissue, the duration values were averaged for the cases with varied body fluid layer thickness. The data is plotted in Fig. 7 and 8 to indicate the main factors responsible for shortening/extending the magnesium concentration in the potentially toxic range and in the therapeutic range.

As seen in Fig. 7, the duration of therapeutic magnesium concentration is rather short, and it is strongly influenced by the thickness of tissue between the implant and capillaries. The initial magnesium concentration in the implant is also a major factor in controlling the duration. The higher the initial magnesium concentration in the implant, the longer the duration of elevated concentration. The implant thickness has moderate effect, and it depends on the tissue thickness and the initial magnesium loading, while the presence of a thin pure PCL coating layer has negligible effect on the duration of therapeutic concentration.

The duration of elevated magnesium concentration is also strongly dependent on the location within the tissue. Several fold shorter durations are seen in the center of the tissue layer as compared the surface facing the implant.

The magnesium concentration exceeding the optimum level is restricted to a few minutes only as seen in Fig. 8. The excessively high concentration is extended if thicker tissue layer is present or when higher initial magnesium loading is applied in the implant. A very significant effect is seen due to the application of a pure PCL layer on the implant which can reduce or eliminate the duration when magnesium concentration is too high. Implant thickness has no effect on the duration of excess magnesium level in the investigated range.

Although, the simulation provided clear insights into the temporal and spatial evolution of magnesium concentration in the vicinity of a magnesium releasing implant, it must be highlighted that there are several shortcomings of the simple model used. Some of these limitations include the assumption of homogeneous tissue layer instead of a cellular structure, the uncertainty of the diffusion coefficients used, and assumption of a purely diffusional magnesium transport between implant and capillaries when there is also possibility of active transport of magnesium into and out of cells, as well as storage of some of the magnesium in the cells. It can also be considered that tissue layers are not solid slabs, but regions separated by small channels where body fluid is present. In such a case, the body fluid may be a fast conduit for magnesium diffusion, thus reducing the overall concentration increase.

In light of the limitations, the results should be taken as semiquantitative that can guide experimental designs on the measurement efficacy of implants or provide a basis for more sophisticated numerical analysis.

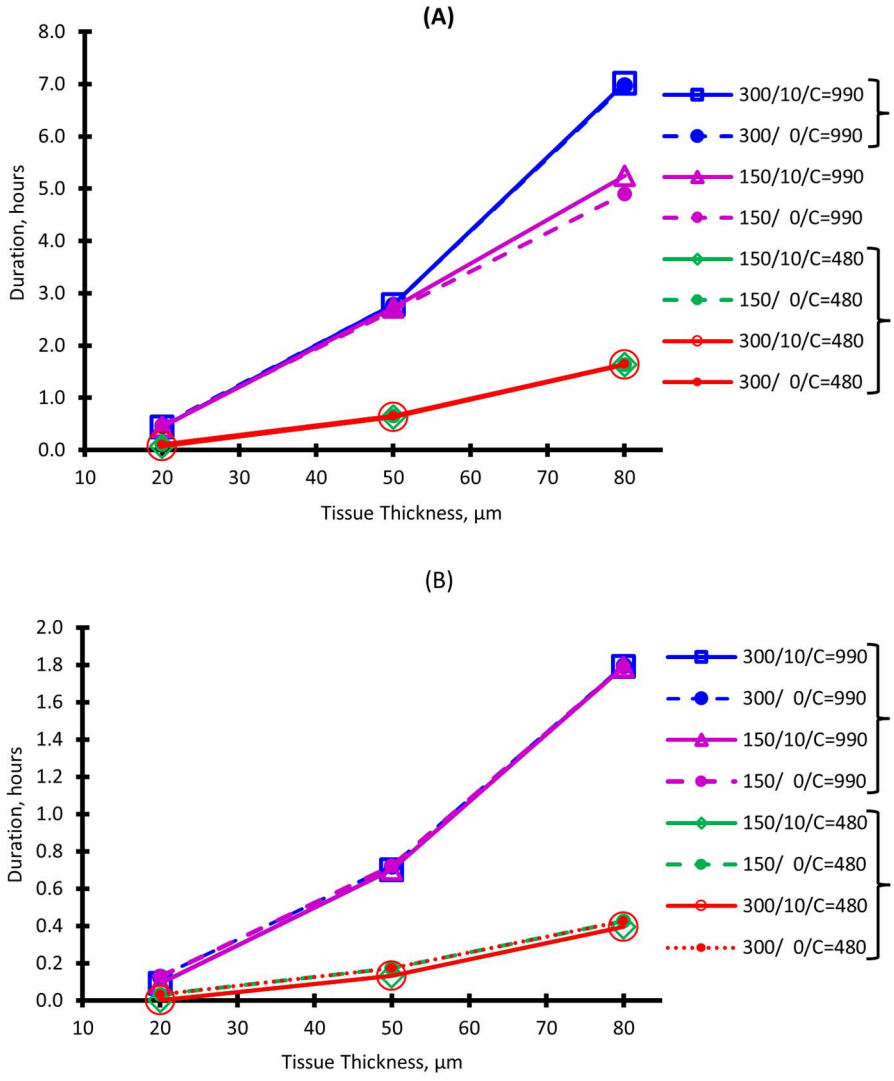

Fig. 7. Duration of Mg^{2+} concentration within the therapeutic range (averaged over varied body fluid layer thickness). Legend: xxx/yy/C=zzz where xxx is the half thickness of the implant, yy is the thickness of pure PCL coating layer, and zzz is the initial Mg^{2+} concentration in the implant in mM; curly brackets indicate data that nearly or fully coincide. (A): Therapeutic Mg^{2+} concentration at the surface of the tissue facing the implant. (B): Therapeutic Mg^{2+} concentration at the center of the tissue layer.

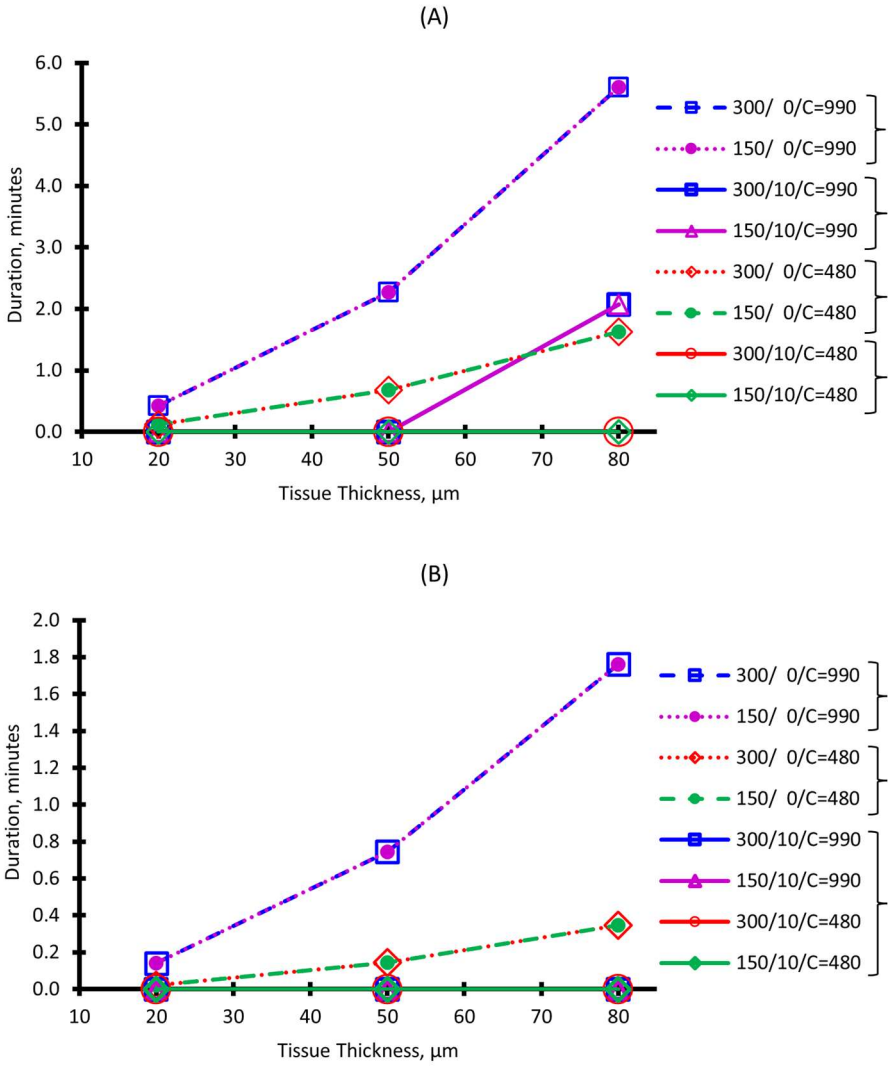

Fig. 8. Duration of Mg^{2+} concentration exceeding the optimum therapeutic range (averaged over varied body fluid layer thickness). Legend: See Fig 7. (A): Excessive Mg^{2+} concentration at the surface of the tissue facing the implant. (B): Excessive Mg^{2+} concentration at the center of the tissue layer.

5 Conclusions

A simple model was set up to numerically evaluate the diffusion controlled release of magnesium sulphate from polycaprolactone implant. The results indicated that the

magnesium is released from the implant at a moderate rate, then it is transported by diffusion across a body fluid layer between implant and tissue at a high rate since the magnesium diffusion coefficient is highest in the body fluid. The subsequent tissue layer with a moderate diffusion coefficient then poses a slight barrier and slows down the diffusion of magnesium.

Two key parameters were identified to describe the efficacy of magnesium release from the implant: The duration of magnesium concentration in the tissue when the magnesium is in the optimum therapeutic range, and the duration where magnesium concentration is above the optimum therapeutic range.

It was found that the duration of optimum magnesium concentration was rather short, well below one day in the scenarios investigated. It can be extended by increasing the initial magnesium loading in the implant, and by using a thicker implant that exhausts its magnesium supply over a longer period. Additionally, the presence of thicker tissue layers between implant and capillaries increased the duration of elevated magnesium concentration in the tissue. On the other hand, the presence of pure polycaprolactone coating had negligible effect on the duration of optimum concentration.

Duration of very high and potentially toxic magnesium levels was found to be short, less than six minutes in all investigated scenarios. This duration is shorter with thinner tissue layers, and for lower initial magnesium loading in the implant. The implant thickness had no effect on this duration but the presence of a pure polycaprolactone coating on the implant had a major effect. Such a coating limits the maximum surface concentration of magnesium in the implant and introduces the magnesium into the body fluid / tissue slower in the initial few minutes.

Thus, the simulation indicated that designing an implant with extended elevated magnesium concentration would rely on high initial magnesium concentration in the implant (>1 M), preferably with thick implants (>600 μm). Additionally, a thin layer of pure polycaprolactone layer (10 to 20 μm) can be applied on the implant to mitigate or prevent the initial magnesium concentration surge when the implant first comes into contact with the tissue.

Overall, it was found that a highly soluble salt such as magnesium sulphate can be incorporated into polycaprolactone implant to achieve elevated magnesium concentration for a limited time period that can promote bone regeneration. Due to the fast clearing of magnesium from the tissue, it was seen that toxic levels of magnesium may be present only for a short time of a few minutes which can be substantially reduced or eliminated by applying a pure PCL layer on the implant.

6 Acknowledgements

This research is supported by A*STAR under its RIE2025 Manufacturing, Trade and Connectivity (MTC) Industry Alignment Fund Industry Collaboration Projects (IAF-ICP) (Award I2101E0010). The support of Osteopore International Pte. Ltd. is also acknowledged.

References

1. De Baaij, J.H.F., Hoenderop, J.G.J., and Bindels, R.J.M.: Magnesium in Man: Implications for Health and Disease. Physiol Rev 95, 1– 46 (2015). DOI:10.1152/physrev.00012.2014
2. Yuan, Z., Wan, Z., Gao, C., Wang, Y., Huang, J., and Cai, Q.: Controlled magnesium ion delivery system for in situ bone tissue engineering. J. Controlled Release 350, 360–376 (2022).
3. Tsai, P.S., Kaufhold, J.P., Blinder, P., Friedman, B., Drew, P.J., Karten, H.J., Lyden, P.D., and Kleinfeld D.: Correlations of Neuronal and Microvascular Densities in Murine Cortex Revealed by Direct Counting and Colocalization of Nuclei and Vessels. The Journal of Neuroscience 29(46), 14553–14570 (2009).
4. Arthur, E., Elsner, A.E., Sapoznik, K.A., Papay, J.A., Muller, M.S., and Burns, S.A.: Distances From Capillaries to Arterioles or Venules Measured Using OCTA and AOSLO. Invest Ophthalmol Vis Sci. 60, 1833–1844 (2019).
5. Nemeth, S., Loke, C.: Drug Release Times from Different Shapes of Releasing Bodies. The 18th International Conference on Biomedical Engineering, 9-12 December 2024, Singapore, Contribution Number: 199 (2024).
6. Crank, J.: The Mathematics of Diffusion. 2nd edn. Clarendon Press, Oxford (1975).
7. Harned, H.S., Hudson, R.M.: The Diffusion Coefficient of Magnesium Sulfate in Dilute Aqueous Solution at 25°. J. Am. Chem. Soc. 73(12), 5880–5882 (1951).
8. Onsager, L., Fuoss, R.M.: Irreversible Processes in Electrolytes, Diffusion, Conductance, and Viscous Flow in Arbitrary Mixtures of Strong Electrolytes, J. Phys. Chem. 36(11), 2689–2848 (1932).
9. Bernengo, J.C., Collet, C., Jacquemond, V.: Intracellular Mg^{2+} diffusion within isolated rat skeletal muscle fibers. Biophysical Chemistry, 89, 35–51 (2001).
10. Ashley, C.C., Ellory, J.C.: The Efflux of Magnesium from Single Crustacean Muscle Fibers. J. Physiol. 226, 653–674 (1972).
11. Baker, P.F., Crawford, A.C.: Mobility and Transport of Magnesium in Squid Giant Axons. J. Physiol. 227, 855–874 (1972).
12. Kalosakas, G., Panagopoulou, P.: Lag Time in Diffusion-Controlled Release Formulations Containing a Drug-Free Outer Layer. Processes 10, 2592 (2022).